U.S. Fish & Wildlife Service

Arcata Fisheries Technical Report TR 2014-19

Development of Two-Dimensional Hydraulic Models to Predict Distribution of *Manayunkia speciosa* in the Klamath River

Katrina A. Wright, Damon H. Goodman, Nicholas A. Som, and Thomas B. Hardy*

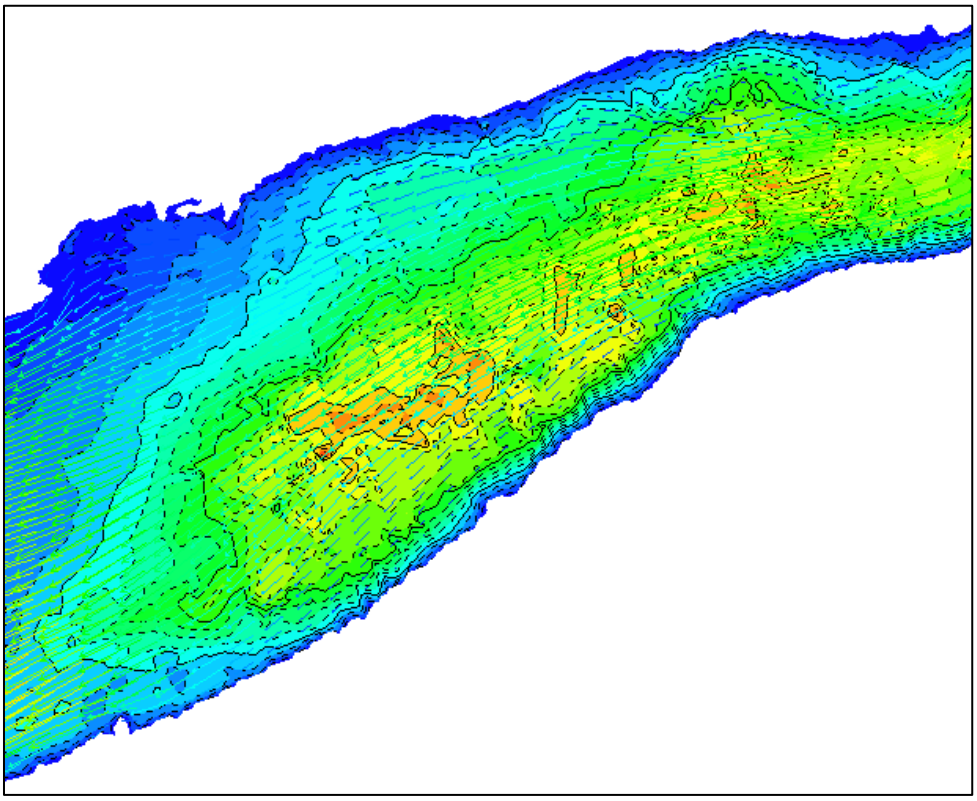

U.S. Fish and Wildlife Service
Arcata Fish and Wildlife Office
1655 Heindon Road, Arcata, CA 95521
(707) 822-7201

**Texas State University*
601 University Drive, San Marcos, TX 78666

January 2014

Funding for this study was provided by the Klamath River Fish Habitat Assessment Program administered by the Arcata Fish and Wildlife Office.

Disclaimer: The mention of trade names or commercial products in this report does not constitute endorsement or recommendation for use by the Federal Government.

The Arcata Fish and Wildlife Office Fisheries Program reports its study findings through two publication series. The **Arcata Fisheries Data Series** was established to provide timely dissemination of data to local managers and for inclusion in agency databases. The **Arcata Fisheries Technical Reports** publishes scientific findings from single and multi-year studies that have undergone more extensive peer review and statistical testing. Additionally, some study results are published in a variety of professional fisheries journals.

key words: Two-Dimensional Hydraulic Model, Calibration, Validation, Klamath River, Fish Disease, Polychaete

The correct citation for this report is:

Wright, K.A., D.H. Goodman, N.A. Som, and T.B. Hardy. 2014. Development of two-dimensional hydraulic models to predict distribution of *Manayunkia speciosa* in the Klamath River. U.S. Fish and Wildlife Service. Arcata Fish and Wildlife Office, Arcata Fisheries Technical Report Number TR 2014-19, Arcata, California.

Table of Contents

List of Tables

List of Tables, continued

List of Figures

List of Figures, continued

page

List of Appendices

Page intentionally blank.

Arcata Fisheries Technical Report TR 2014-19

Development of Two-Dimensional Hydraulic Models to Predict Distribution of *Manayunkia speciosa* in the Klamath River

Katrina A. Wright, Damon H. Goodman, Nicholas A. Som, and Thomas B. Hardy*

U.S. Fish and Wildlife Service, Arcata Fish and Wildlife Office
1655 Heindon Road, Arcata, CA 95521
katrina_wright@fws.gov

**Texas State University, 601 University Drive, San Marcos, TX 78666*

Abstract.—We developed two-dimensional hydraulic models at three study sites in the Klamath River. This report describes the data collection, calibration, and validation performed to build the models and test their performance. The hydraulic models showed excellent agreement between predicted and observed water surface elevations, area of inundation, and spatial distributions of depth and velocity both at calibration and independent validation discharges. Water surface elevations were predicted within an average of 0.048 m at calibration streamflows and 0.076 m at validation streamflows. Water inundation extent was predicted within an average of 0.39 m at calibration streamflows and 0.31 m at validation streamflows. The predicted depth and velocity patterns generally matched observed data, with 90% of predicted depths within 0.15 m of observed values and 90% of predicted velocities within 0.45 m/s of observed values. Fine-scale velocity, depth, and shear stress predictions computed by the hydraulic models will be used to develop habitat preference models for *Manayunkia speciosa*, the freshwater polychaete that is an intermediate host for the salmonid parasite *Ceratomyxa shasta*. This information will allow scientists to evaluate whether flow manipulation is a potentially viable management action to impair hydraulic habitat and disrupt the disease cycle.

Introduction

Ceratomyxosis is an infectious disease caused by the myxozoan parasite *Ceratomyxa shasta*, which has a complex life-cycle involving both salmonids and an intermediate invertebrate host species, the freshwater polychaete worm *Manayunkia speciosa* (Bartholomew et al. 1997; Bartholomew et al. 2006). In the past decade the effect of ceratomyxosis on Klamath River salmon populations has become a fisheries management concern. Out-migrating juvenile Chinook salmon are experiencing

significant disease infection and mortality (True et al. 2013), with negative impacts on adult escapement (Fujiwara et al. 2011). Scientists are currently investigating strategies to reduce *M. speciosa* abundance and in turn disease prevalence in salmonids. One possible approach is to decrease polychaete abundance by limiting their preferred habitats or disrupting their lifecycle through streamflow management. However, we must first understand their distribution and abundance as it relates to their physical environment and the hydraulics of the Klamath River.

The habitat preferences of *M. speciosa* in the Klamath River are not well understood. Previous studies in the Klamath River have found them in a variety of microhabitats, in particular, low velocity conditions, associated with periphyton (*Cladophora* sp.) and aquatic vegetation, and on substrate grain sizes ranging from sand to bedrock (Stocking and Bartholomew 2007; Wilzbach and Cummins 2009; Jordan 2012; Malakauskas and Wilzbach 2012). Two of these studies have indicated that polychaete distribution is affected by the stability of their microhabitat environment during high streamflows that may occur in winter and spring months. Stocking and Bartholomew (2007) noted that a dense population of polychaetes in sand-silt was absent following a high discharge event, and speculated that distribution is influenced by flow-mediated microhabitat stability. This hypothesis is supported by Jordan (2012), who found that summer-time polychaete densities decreased within specific feature types (i.e. run, riffle, pool) following a high streamflow. A predictive model for *M. speciosa* density was developed by Jordan (2012) that included depth, velocity, and substrate size, but it poorly predicted *M. speciosa* density in the subsequent year following a high streamflow, possibly due to the lack of a variable describing flow history.

We plan to build on the current understanding of *M. speciosa* habitat preferences by incorporating flow history through application of two-dimensional hydraulic modeling. Hydraulic models can simulate the conditions experienced at the microhabitat-scale over a wide range of discharges. They will allow us to predict the depth, velocity, and shear stress occurring during high streamflows and evaluate the effect of streamflow on polychaete habitat. In coordination with Oregon State University we have implemented this study with the goals of (1) building spatially explicit hydraulic models that predict the hydraulic conditions experienced by a polychaete at a specific location, and (2) rigorously sampling the distribution and abundance of polychaetes over the range of available depth, velocity, and substrate grain sizes to better inform habitat preference models. All polychaete observations will be spatially georeferenced so that they can be associated with hydraulic model-predicted streamflow conditions. After the development of the habitat preference model, the hydraulic models will allow us to predict the distribution of polychaetes over the spatial extent of the study sites.

This report describes the hydraulic model development process of data collection, model calibration, and model validation. We developed hydraulic models at three study sites on the Klamath River to provide predictions of depth, velocity, shear stress, and substrate size at the microhabitat scale across the entire river channel over

a range of streamflows. The second goal of this effort, polychaete habitat preference modeling, is currently on-going and will be the subject of a future publication.

Methods

Study sites

The Klamath River watershed encompasses approximately 26,000 km^2 in California and 14,000 km^2 in Oregon. It is divided into upper and lower basins by a series of six irrigation and hydropower dams. Iron Gate Dam is the closest dam to the ocean and a barrier to upstream passage of anadromous salmonids. It is located at 310.3 river kilometers (rkm) upstream of the river mouth near the California-Oregon State border. The largest tributaries in the basin join with the main-stem river downstream of Iron Gate Dam and include the Trinity, Salmon, Scott, and Shasta rivers.

Three study sites were located on the main-stem Klamath River between its confluences with the Shasta and Scott rivers (Figure 1). Modeled sites were located near the Tree of Heaven Campground (rkm 281; 0.43 km long), Beaver Creek (rkm 264; 0.83 km long), and Klamath Community Center (rkm 259; 1.38 km long). These sites were selected because they were known to host polychaetes (Stocking and Bartholomew 2007; Jordan 2012; Malakauskas and Wilzbach 2012), and because they lay within sections of the river known to be sources of disease transmission (Hallett et al. 2012).

Hydraulic model

The USGS Multi-Dimensional Surface-Water Modeling System (MD_SWMS) Flow and Sediment Transport and Morphological Evolution of Channels (FaSTMECH) computational model was used to simulate water-surface elevation, water depth, depth-averaged water velocity, and bed shear stress (McDonald et al. 2005, 2006). This model solves steady-state, depth-averaged Navier-Stokes equations, which are the governing equations of fluid motion expressing the principle of conservation of momentum in fluid flow. These equations are solved at each node of a user-defined computational curvilinear mesh. We created computational meshes for each site with node spacing of approximately 0.5 m by 0.5 m at the Tree of Heaven and Beaver Creek sites, and 0.75 m by 0.75 m at the Community Center site. The Community Center site was much larger than the other two, and computational constraints dictated wider node spacing. At each cell node, the hydraulic model computes stream flow characteristics (for example, depths, velocities, and shear stresses) as a function of discharge and channel geometry. FaSTMECH requires input data of site topography, a stage-discharge relationship describing the boundary conditions, water surface elevations for calibration, and spatially delineated bed roughness height in terms of substrate grain size and vegetation type.

Data collection

Model input data

Topographic data were collected using Trimble (Trimble Navigation Limited, Sunnyvale, California) R8 real-time kinematic (RTK) global positioning system (GPS), Topcon (Topcon Positioning Systems Incorporated, Livermore, California) Hiper+ RTK GPS, SonarMite (Ohmex Limited, Sway, Hampshire, United Kingdom) echo sounder, and Sokkia (Sokkia Corporation, Olathe, Kansas) Powerset 3000 total station. The error tolerance for RTK data collection was approximately ±0.03 m. All data were recorded in Universal Transverse Mercator (Zone 10 North) coordinates using the North American Datum of 1983 and the North American Vertical Datum of 1988 (Geoid09). We established local survey control benchmarks at each site using RTK GPS positioning with a base station set on National Geodetic Survey control stations (Beaver MX1307, Third Vertical Order; Humbug MX1318, Second Horizontal Order). Surveyed data were supplemented with an existing airborne light detection and ranging (LiDAR) dataset collected in 2010 (Woolpert Inc. 2010). Topographic point density ranged from 0.23 to 0.36 points/m^2 over each site (Table 1), with higher point densities within the base flow wetted channel (0.43 to 0.55 points/m^2) than on the overbank areas (0.16 to 0.20 points/m^2). Figures in Appendix A show spatial density by survey point type within each study site.

We constructed a digital elevation model (DEM) of each study site using the Delauney Triangulated Irregular Network (TIN) algorithm to interpolate between survey points (Appendix B). Triangulation anomalies were removed by visual inspection within ArcGIS and ArcScene software (Esri, Redlands, California). Most DEM anomalies were caused by specious echo sounder readings in shallow or turbulent water, or were due to inaccurate LiDAR measurements along the water's edge. An area of the Beaver Creek study site was not surveyed due to dangerous water conditions (Appendix A-2). This data gap was rectified through topographic interpolation along feature lines; break lines were drawn to connect measured points and produce elevation contours consistent with river features.

Substrate size and vegetation type were mapped over the extent of each study site using GPS (ProXH with zephyr antenna, Trimble Navigation Limited, Sunnyvale, California) and merged to create variable roughness input for the hydraulic model. The error tolerance for GPS data collection was approximately ±1.2 m. Visual estimates of substrate grain size were made by snorkel and scuba observation (Appendix C). Median substrate secondary diameter (D50) was visually estimated to the closest millimeter at each observation location. Observation density was related to D50 size gradients, with more observations recorded in areas with higher gradients. Observation point density ranged from 0.011 to 0.018 points per m^2 by site (Table 2). Figures showing survey point distribution and the spatial distribution of substrate size categories over the sites are included in Appendix C. The hydraulic model roughness input consists of the continuous metric of D50 values, but a modified Wentworth scale was used to categorize substrate measurements for illustrative purposes (Table 3, Wentworth 1922). Silt and sand were collapsed into a single category due to observers' inability to measure grain size < 2 mm in diameter.

Patches of fines (< 2 mm), large boulders (> 1.5 m diameter), and bedrock were mapped as polygons. Observations of substrate size (D50) in the gravel, cobble, and small boulder categories were interpolated using the Delauney TIN method to provide a map of the entire site.

In-river and bank vegetation were also mapped in the field using GPS (Appendix D). Polygons were drawn around vegetation types and each polygon was assigned a metric roughness height based upon type and density (Table 4; Hardy et al. 2006; modification to metric roughness from T.B. Hardy, pers. comm. 2011). Substrate and vegetation roughness maps were combined to create an overall spatial roughness map of each site. In locations where vegetation and substrate observations overlapped, the greater roughness value was used. This process resulted in a layer of georeferenced variable roughness heights within each site for use in the hydraulic model calibrations.

Flow boundary conditions were measured at three or more streamflows at each site (Table 5). At all flow levels, we measured discharge at the upstream boundary with a Rio Grande acoustic Doppler current profiler (ADCP; Teledyne RD Instruments, Poway, California) attached to a slow-moving boat. We collected consecutive cross-sectional discharge measurements until we had five measurements within 5% of each other. The final discharge estimate was an average of these five measurements. At each flow level the corresponding stage height was recorded with RTK GPS at the downstream site boundary. Recorded measurements were used as inputs for the calibration and validation simulations. Log-linear stage-discharge relationships were produced for each site to estimate input stage height conditions for simulations at a variety of discharges (Appendix E).

Hydraulic data for model calibration and validation

Hydraulic datasets were collected at the discharges shown in Table 5 and used for either model calibration or validation. These data included water surface elevation (WSE) profiles, water's edge locations, depths, and velocities. We validated the models with independent data collected at the highest sampling discharges to test their ability to extrapolate beyond the calibration data.

Two methods were used to survey the WSE profiles in the field. WSE was measured in the middle of the channel by attaching an RTK GPS to a boat at a known distance above the water and floating the thalweg of the river while recording continuous measurements, capturing the WSE profile in the center of the channel (hereafter referred to as "thalweg water surface"). WSE was also measured at the water's edge along the length of each study reach (hereafter referred to as "water's edge points"). Both survey methods were used to record WSE at each sampling discharge with one exception: only water's edge points were collected at the Beaver Creek site at 130.55 cms because sampling time was limited.

Models were calibrated at the calibration discharges by adjusting each site's variable roughness height via a multiplier until the predicted water surface elevations

matched observed water surface elevations. The difference between predicted and observed water surfaces was evaluated by the root mean square error (RMSE). Lateral eddy viscosity and water surface drag coefficient input parameters were also adjusted to improve model fit. Hydraulic model input parameters for each calibration flow at each site are presented in Table 6. Calibrated models were run for 6,000 or more iterations and converged with less than one percent mean error in the computed versus simulated discharge.

After the model input parameters were calibrated, a secondary model calibration step consisted of comparing the predicted water inundation extent to the observed water's edge locations. We compared the horizontal position of the predicted and observed water's edge points for each calibration discharge through each study reach. To put the magnitude of these differences in perspective, we calculated each site's mean channel width at each discharge by dividing the predicted wetted area by the site length.

For model validation, two of the models were evaluated at independent discharges not used for calibration (149.99 cms for Tree of Heaven site model; 130.55 cms for Beaver Creek site model). The roughness coefficients for these simulations were estimated with log-linear relationships of the calibrated parameter values and calibration discharges for each site. Lateral eddy viscosities and water surface drag coefficients were estimated using the same method. The hydraulic model input parameters for validation simulations are presented in Table 6. Predictions at validation discharges were compared with measured field data. Measured data included vertical WSE profiles and water's edge locations at the Tree of Heaven and Beaver Creek sites.

An additional validation of model performance was considered by comparing the predicted and observed depths and velocities at all three sites. At every discharge we measured multiple cross-sectional depth and depth-averaged velocity profiles with an ADCP attached to a slow-moving boat. Cross sections were distributed along the extent of each study site to capture the position of the thalweg and eddy separation lines at each discharge. See figures in Appendix F for transect locations. Predicted values were compared with observed depth and velocity magnitudes. The range of predictions within the immediate vicinity of each measurement location was used for comparison with the measured value given the known measurement uncertainty in the observation location versus computational grid locations. Therefore, predicted values located within 0.7 m of the observed value's location were used for comparison at the sites with 0.5 m computation grid spacing (Tree of Heaven and Beaver Creek sites), and predicted values located within 1 m of the observed value's location were used for comparison at the 0.75 m computational gridded site (Community Center site). To incorporate the range of predicted values, residuals were calculated by subtracting either the maximum or minimum predicted value from the observed data.

Results

The hydraulic models were evaluated by comparing predictions of WSE, water inundation, depth, and velocity with observed measurements at calibration and validation discharges. The model predicted WSE profiles that matched the observed WSE profiles very well along the modeled reaches, and captured slope changes at hydraulic drops (Figures 2-4). The models were calibrated to predict WSE within an average of 0.048 m of the measured values at calibration streamflows (Table 7). The models exhibited slightly higher errors in predicting WSE at independent validation discharges. Predicted WSE were within 0.072 or 0.077 m of measured WSE depending on thalweg versus water's edge WSE comparisons at Tree of Heaven, and within 0.080 m of measured values at Beaver Creek (Table 7). The thalweg WSE model predictions matched observations better than water's edge WSE predictions for all sites and discharges except at Community Center at 33.89 cms.

There was an unstable hydrograph during validation data collection and the discharge at the Tree of Heaven site dropped approximately 5% over the measurement period. The change in observed WSE is apparent in Figure 2 "Validation 149.99 CMS, Thalweg Float Data." When model fit was evaluated by a subset of data collected early in the sampling period, the predictions were within 0.044 m of the observed data (Table 7). Although the predicted data were higher than the latter subset of WSE observations (RMSE = 0.082 m; Table 7), the model predictions tracked the longitudinal profile pattern (Figure 2). The Beaver Creek validation measurements taken on the same day were collected in a shorter time period, and were not as affected by changes in discharge.

All three models performed well based on a comparison of predicted and observed water inundation extent. At calibration discharges, the predicted water's edge averaged 0.39 m horizontal distance from the observed water's edge (Table 8). This magnitude of difference represented, on average, 0.9% of the mean channel width. At validation discharges, the horizontal distance between predicted and observed water's edge decreased to an average of 0.31 m (0.7% of the mean channel width). The greatest maximum differences occurred at the Community Center site at the 73.07 and 113.15 cms streamflows where predicted water's edges were 2.81 and 4.52 m away from the observed locations, representing 6.0 and 8.9% of the mean channel width, respectively. This magnitude of error was rare in the dataset.

Model performance in terms of predicted depth and velocity was evaluated for each discharge. The moving-boat ADCP transect locations are provided in Appendix F. Comparison plots of predicted and observed depths and velocities for each transect are provided in Appendix G. Predicted depths closely tracked observed values. The shape of predicted and observed velocity distributions across the channel matched fairly well, with the observed values generally displaying scatter around the predicted values. Histograms and cumulative density distributions of depth and velocity residuals are shown in Figures 5 and 6. Overall, the hydraulic models predicted depth better than velocity. Ninety-percent of predicted depths were within 0.15 m of the observed depth, and 90% of predicted velocities were within 0.45 m/s of measured velocities. The velocity prediction

errors varied by site and calibration/validation dataset (Figure 7) and discharge magnitude between study sites (Figure 8). Median residuals at all sites and discharges were near zero, except for the validation streamflow at Tree of Heaven (149.99 cms) that had a slight negative bias (median residual = -0.19 m/s). The predicted velocities at this discharge were higher than the observed velocities.

Discussion

The hydraulic models developed at three study sites on the Klamath River were calibrated and validated. The models showed good agreement between predicted and observed water surface elevations. Predicted water surface elevations for calibration discharges were within an average of 0.048 m from the observed values, an acceptable magnitude of error considering the ±0.03 m vertical precision of the measured data, and comparable to values reported by other studies. For example, Hardy et al. (2006) matched water surface elevations generally within 0.05 m for hydraulic model calibration, and Legleiter et al. (2011) matched water surface elevations within 0.035 m. Our models exhibited slightly higher errors in predicting water surface elevations at the extrapolated validation discharges. They predicted water surface elevations within 0.072 to 0.080 m at validation discharges of 149.99 cms at Tree of Heaven and 130.55 cms at Beaver Creek. This error was within acceptable limits and was due in part to field measurements taken during unstable streamflows. Model-simulated water inundation extent fit observed water's edge data at all discharges.

Similar to other findings, the hydraulic models predicted depth better than velocity (Pasternack et al. 2006; Waddle 2010). Velocity errors in hydraulic model predictions commonly averaged 20 to 30% (Pasternack et al. 2006; Waddle 2010; Legleiter et al. 2011), and were attributed to uncertain topographic input and computational mesh coarseness. Although differences were noted between our predicted and measured velocities, the magnitude and structure of flow across the cross-sections were simulated well. The comparatively smooth nature of the predicted velocities was in part due to velocities being computed as the depth-averaged values based on channel topography. The instantaneous nature of the ADCP measurements also accounted for some of the scatter of the observed data around the predicted values. Collecting depth-averaged velocity measurements from a moving boat allowed us to gain a larger breadth of data across the site, and we found that the models correctly predicted the position of the thalweg and eddy separation lines at the study sites.

One exception to this was a section at Beaver Creek at 32.49 cms, where the model predicted the thalweg occurring 10 m away from its observed location (Appendices G-72 and G-73). Legleiter et al. (2011) found that using uncertain input topography led to errors in the model predictions, especially if topography was incorrect on point bars or in high gradient areas where channel geometry drove flow patterns. This could explain the poor predictions, since these transects were located where the channel makes a sharp bend downstream of a point bar. Perhaps the topography was

not surveyed densely enough to capture the true channel topography in the computational grid. However, the model performed better at predicting the thalweg location in this section at higher flow levels (Appendices G-85, G-86, G-105, and G-106). When Legleiter et al. (2011) compared model uncertainty between different streamflows, they also found that the modeled flows exhibited less sensitivity to errors in topography at discharges above base flow.

Hydraulic model development was the first objective in this joint study with Oregon State University. The calibrated and validated hydraulic models at these three study sites will be used to simulate physical hydraulic characteristics (i.e. depth, velocity, shear stress, and substrate size) over a range of target flow levels. This will allow us to predict the conditions experienced by polychaetes during winter and spring high streamflows when it is not feasible to collect field observations. The second objective of our joint study is to intensively survey polychaete distribution and abundance at these sites and build relationships between georeferenced observations and hydraulic habitat variables. The hydraulic models and habitat preference models will be used in combination to investigate the viability of manipulating flow to create disturbance and limit the abundance of polychaete habitat. These models will further our understanding of polychaete-habitat interactions and help guide future water management decisions made to decrease polychaete populations, decrease *C. shasta* infectivity rates within polychaete populations, and reduce the prevalence of ceratomyxosis in juvenile salmonid stocks in the Klamath Basin.

Acknowledgements

The Arcata Fish and Wildlife Office wishes to acknowledge Michelle Jordan, former graduate student in Dr. Jerri Bartholomew's Salmon Disease Lab at Oregon State University, for her initiation of this project and her help in data collection. This report is part of a collaborative fish disease study, and this work would not have been possible without the field support of members of the Salmon Disease Lab and other members of our office. We also thank the Yurok Tribe Fisheries Department for their assistance during the February 2011 Iron Gate Dam pulse flow event.

Literature Cited

Bartholomew J.L., S.D. Atkinson, S.L. Hallett. 2006. Involvement of *Manayunkia speciosa* (Annelida: Polychaeta: Sabellidae) in the life cycle of *Parvicapsula minibicornis*, a myxozoan parasite of Pacific Salmon. Journal of Parasitology 92: 742-748.

Bartholomew, J.L., M.J. Whipple, D.G. Stevens, and J.L. Fryer. 1997. The life cycle of *Ceratomyxa shasta*, a myxosporean parasite of salmonids, requires a freshwater polychaete as an alternate host. Journal of Parasitology 83(5): 859-868.

Fujiwara, M. M.S Mohr, A. Greenberg, J.S. Foott, and J.L. Bartholomew. 2011. Effects of ceratomyxosis on population dynamics of Klamath fall-run Chinook salmon. Transactions of the American Fisheries Society 140(5): 1380-1391.

Hallett, S.L., R.A. Ray, C.N. Hurst, R.A. Holt, G.R. Buckles, S.D. Atkinson, and J.L Bartholomew. 2012. Density of waterborne parasite *Ceratomyxa shasta* and its biological effects on salmon. Applied and Environmental Biology 78(10): 3724-3731.

Hardy, T.B., R.C. Addley, and E. Saraeva. 2006. Evaluation of instream flow needs in the lower Klamath River, Phase II, Final Report. Prepared for the U.S. Department of the Interior. Institute for Natural Systems Engineering, Utah Water Research Laboratory, Utah State University, Logan, Utah.

Jordan, M. 2012. Hydraulic predictors and seasonal distribution of *Manayunkia speciosa* density in the Klamath River, CA, with implications for ceratomyxosis, a disease of salmon and trout. Master of Science Thesis. Oregon State University, Corvallis, Oregon.

Legleiter, C.J., P.C. Kyriakidis, R.R. McDonald, and J.M. Nelson. 2011. Effects of uncertain topographic input data on two-dimensional flow modeling in a gravel-bed river. Water Resources Research 47.

Malakauskas, D.M. and M.A. Wilzbach. 2012. Invertebrate assemblages in the lower Klamath River, with reference to *Manayunkia speciosa*. California Fish and Game 98(4): 214-235.

McDonald, R.R., J.M. Nelson, and J.P. Bennett. 2005. Multi-dimensional surface-water modeling system user's guide. U.S. Geological Survey Techniques and Methods, 6-B2,136 p.

McDonald, R.R., J.M. Nelson, P.J. Kinzel, and J.S. Conaway. 2006. Modeling surface-water flow and sediment mobility with the multi-dimensional surface water modeling system. U.S. Geological Survey Fact Sheet 2005-3078.

Pasternack, G.B., A.T. Gilbert, J.M. Wheaton, and E.M. Buckland. 2006. Error propogation for velocity and shear stress prediction using 2D models for environmental management. Journal of Hydrology 328: 227-241.

Stocking, R.W. and J.L. Bartholomew. 2007. Distribution and habitat characteristics of *Manayunkia speciosa* and infection prevalence with the parasite *Ceratomyxa shasta* in the Klamath River, Oregon-California. Journal of Parasitology 93(1): 78-88.

True, K., A. Bolick and J.S. Foott. 2013. FY 2012 Investigational report: Myxosporean Parasite (*Ceratomyxa shasta* and *Parvicapsula minibicornis*) annual prevalence of infection in Klamath River Basin juvenile Chinook salmon, April-August 2012. U.S. Fish & Wildlife Service California – Nevada Fish Health Center, Anderson, CA.

Waddle, T. 2010. Field evaluation of a two-dimensional hydrodynamic model near boulders for habitat calculation. River Research and Applications 26: 730-741.

Wentworth, C.K. 1922. A scale of grade and class terms for clastic sediments. Journal of Geology 30(5): 377-392.

Wilzbach, M.A. and K.W. Cummins. 2009. Recommendations for study of the distribution and population dynamics of the freshwater polychaete, *Manayunkia speciosa* in the lower Klamath River. USGS Research Work Order 77, Final Report February 2009.

Woolpert, Inc. 2010. Klamath River LiDAR and Mapping, 2010: Link River Dam, OR to the confluence with Elk Creek south of Happy Camp, CA. U.S. Bureau of Reclamation Contract No: 08-CA-40-8258, Task Order: R10PD40007.

Table 1. Topographic data points for the three study sites on the Klamath River. Point counts and densities are tabulated by area for the baseflow channel, the overbank area, and the total site. Density values are given in m^{-2}. Spatial distributions of observations by type and across site are shown in Appendix A.

	Base flow channel		Overbank area		Total	
Site	n	Density (m^{-2})	n	Density (m^{-2})	n	Density (m^{-2})
Tree of Heaven	6,725	0.43	6,806	0.20	13,531	0.28
Beaver Creek	17,354	0.55	5,340	0.17	22,694	0.36
Community Center	25,251	0.43	28,545	0.16	53,796	0.23

Table 2. Observations of substrate particle size at the three study sites on the Klamath River. Density values are reported in m^{-2}. Spatial distributions of observations across study sites are shown in Appendix C.

Site	n	Density (m^{-2})
Tree of Heaven	331	0.018
Beaver Creek	554	0.014
Community Center	793	0.011

Table 3. The modified Wentworth scale used to classify D50 grain size into substrate classes (Wentworth 1922).

Substrate class	D50 grain size (mm)
Silt/Sand	< 2
Gravel	2 - 64
Cobble	64 - 256
Boulder	256 – 5,000
Bedrock	> 5,000

Table 4. Roughness heights assigned to vegetation types mapped at the three study sites on the Klamath River (modified from Hardy et al. 2006; pers. comm. T.B. Hardy 2011). Roughness height values are in meters, and vary by vegetation density (dense or sparse).

	Roughness height (m)	
Vegetation type	Dense	Sparse
Aquatic Non Emergent	0.07	0.07
Aquatic Emergent	1.2	0.6
Grass	0.23	0.07
Grape Vines	1.2	0.23
Willows	1.2	0.23
Berry Vines	1.2	0.23
Trees <4" Diameter at Breast-Height (dbh)	0.6	0.23
Trees >4" dbh	0.6	0.23
Aggregates of Small Vegetation (<4" in height)	1.2	0.23
Aggregates of Large Vegetation (>4" in height)	1.2	0.23

Table 5. Sampling date, discharge (Q), stage, and data type (calibration or validation) of hydraulic datasets collected at three study sites on the Klamath River located at Tree of Heaven, Beaver Creek, and Community Center.

Site	Sampling Date	Q (cms)	Stage (m)	Calibration	Validation
Tree of Heaven	8/17/2011	33.33	589.782	x	
Tree of Heaven	6/29/2011	57.33	590.059	x	
Tree of Heaven	4/12/2011	116.22	590.528	x	
Tree of Heaven	2/10/2011	149.99	590.667		x
Beaver Creek	8/15/2011	32.49	532.599	x	
Beaver Creek	6/27/2011	57.37	532.832	x	
Beaver Creek	4/13/2011	111.54	533.234	x	
Beaver Creek	2/10/2011	130.55	533.290		x
Community Center	8/16/2011	33.89	518.901	x	
Community Center	6/28/2011	73.07	519.199	x	
Community Center	4/14/2011	113.15	519.407	x	

Table 6. Model input parameters for calibration and validation model runs at three study sites on the Klamath River: Tree of Heaven, Beaver Creek, and Community Center. Data type is calibration (C) or validation (V). Input parameters include discharge at upstream boundary (Q; cms), stage height at downstream boundary (m), roughness coefficient (m), lateral eddy viscosity (LEV; m^2/s), water surface elevation (WSE; m) drag coefficient, relaxation coefficients, and number of model iterations.

Site	Data Type	Q (cms)	Stage (m)	Roughness Coeff. (m)	LEV (m^2/s)	WSE Drag Coeff.(m)	Relaxation Parameters	Model Iterations
Tree of Heaven	C	33.33	589.78	0.120	0.090	0.0015	0.3, 0.5, 0.5	7,000
Tree of Heaven	C	57.33	590.06	0.090	0.100	0.0030	0.3, 0.5, 0.5	7,000
Tree of Heaven	C	116.22	590.53	0.065	0.115	0.0050	0.3, 0.5, 0.5	7,000
Tree of Heaven	V	149.99	590.67	0.057	0.121	0.0067	0.3, 0.5, 0.5	7,000
Beaver Creek	C	32.49	532.60	0.080	0.050	0.0050	0.7, 0.6, 0.6	7,000
Beaver Creek	C	57.37	532.83	0.100	0.071	0.0120	0.7, 0.6, 0.6	7,000
Beaver Creek	C	111.54	533.23	0.130	0.100	0.0300	0.7, 0.6, 0.6	7,000
Beaver Creek	V	130.55	533.29	0.138	0.110	0.0383	0.7, 0.6, 0.6	7,000
Community Center	C	33.89	518.90	0.090	0.050	0.0300	0.2, 0.3, 0.3	7,000
Community Center	C	73.07	519.20	0.050	0.120	0.0150	0.2, 0.3, 0.3	7,000
Community Center	C	113.15	519.41	0.040	0.200	0.0090	0.2, 0.3, 0.3	6,000

Table 7. Comparison of model-predicted and observed water surface elevation at study sites on the Klamath River: Tree of Heaven, Beaver Creek, and Community Center. Data type is calibration (C) or validation (V). Two sets of observed water surface elevation data are compared with model predictions: (1) thalweg water surface, and (2) water's edge points. The difference between predicted and observed data is evaluated by root mean square error (RMSE).

Site	Data Type	Q (cms)	Thalweg Water Surface		Water's Edge Points	
			n	RMSE (m)	n	RMSE (m)
Tree of Heaven	C	33.33	1269	0.019	45	0.042
Tree of Heaven	C	57.33	1143	0.018	44	0.066
Tree of Heaven	C	116.22	1267	0.028	99	0.056
Tree of Heaven	V	149.99	622	0.072	61	0.077
Tree of Heaven	V	149.99	(199*)	(0.044*)		
Tree of Heaven	V	149.99	(423**)	(0.082**)		
Beaver Creek	C	32.49	2848	0.029	97	0.048
Beaver Creek	C	57.37	2591	0.027	165	0.065
Beaver Creek	C	111.54	1955	0.039	143	0.069
Beaver Creek	V	130.55	NA	NA	60	0.080
Community Center	C	33.89	2715	0.053	71	0.036
Community Center	C	73.07	2619	0.057	81	0.080
Community Center	C	113.15	2631	0.050	59	0.083

* Portion of data collected at beginning of sampling period.
** Portion of data collected at end of sampling period.

Table 8. Comparison of model-predicted and observed water's edge locations at three study sites on the Klamath River: Tree of Heaven, Beaver Creek, and Community Center. Data type is calibration (C) or validation (V).

Site	Data Type	Q (cms)	Mean Channel Width (m)	Distance Between Predicted and Observed				
				n	Mean (m)	Min (m)	Max (m)	SD (m)
Tree of Heaven	C	33.33	36.2	48	0.37	0.00	0.97	0.23
Tree of Heaven	C	57.33	38.1	44	0.32	0.02	1.00	0.21
Tree of Heaven	C	116.22	41.6	99	0.49	0.03	2.27	0.35
Tree of Heaven	V	149.99	42.7	63	0.26	0.01	0.83	0.20
Beaver Creek	C	32.49	38.0	97	0.32	0.02	1.70	0.28
Beaver Creek	C	57.37	39.7	166	0.28	0.00	1.88	0.27
Beaver Creek	C	111.54	42.9	142	0.25	0.00	1.70	0.22
Beaver Creek	V	130.55	43.7	62	0.37	0.05	1.48	0.23
Community Center	C	33.89	42.7	71	0.42	0.01	1.38	0.29
Community Center	C	73.07	47.2	85	0.49	0.02	2.81	0.57
Community Center	C	113.15	50.7	106	0.64	0.03	4.52	0.61
Calibration, combined				858	0.39	0.00	4.52	0.39
Validation, combined				125	0.31	0.01	1.48	0.22
All				983	0.38	0.00	4.52	0.37

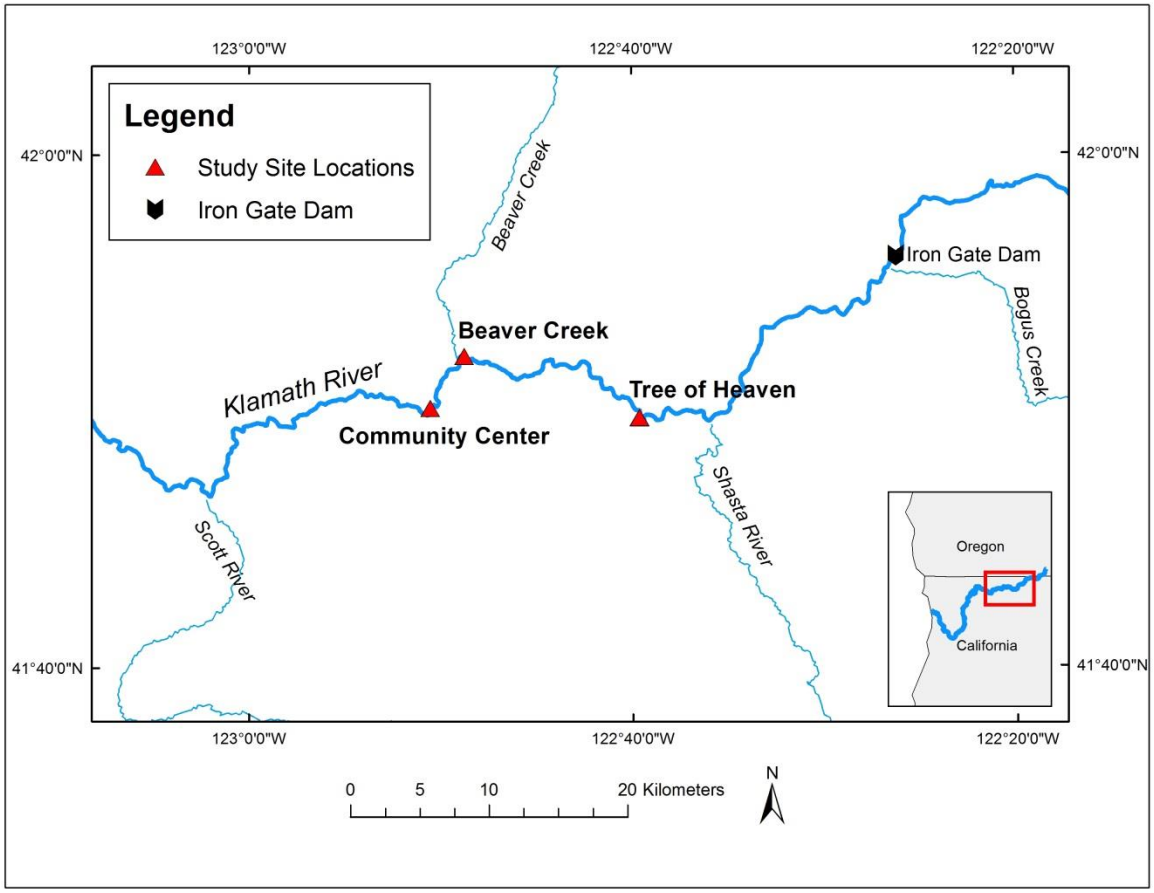

Figure 1. We developed two-dimensional hydraulic models at three study sites on the Klamath River between its confluences with the Shasta and Scott Rivers. Modeled sites are located at the Tree of Heaven Campground (rkm 281; 0.43 km long), Beaver Creek (rkm 264; 0.83 km long), and Klamath Community Center (rkm 259; 1.38 km long)

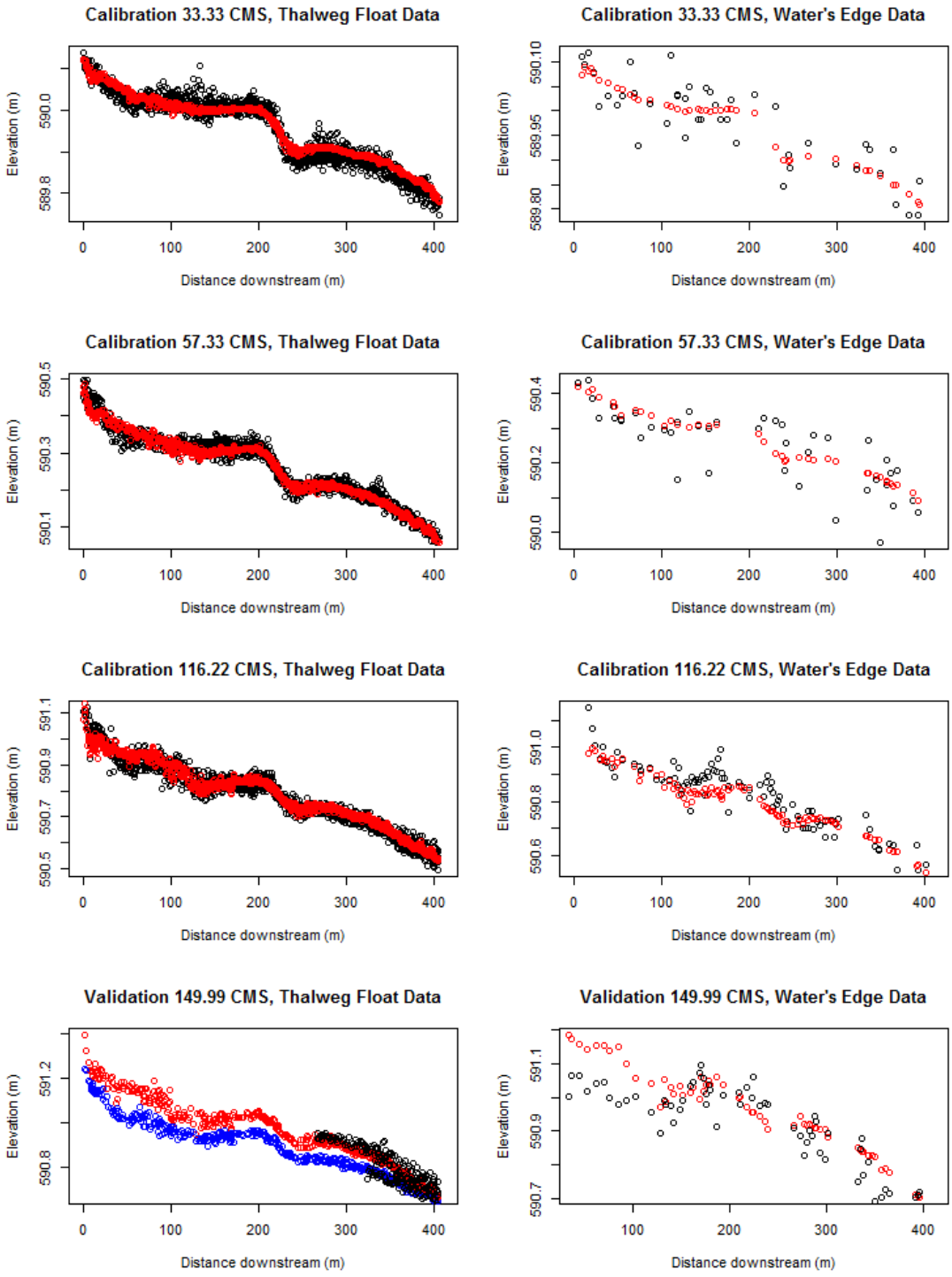

Figure 2. Longitudinal water surface elevation (WSE) plots comparing predicted (red) with observed (black) values at four discharges (33.33, 57.33, 116.22, and 149.99 cms) at the Tree of Heaven study site. Model predictions are compared with two sets of observed WSE data: (1) thalweg water surface (L column), and (2) water's edge points (R column). In the validation plot of thalweg data at 149.99 cms, the observed values are divided by time: early in sampling period (black), and later in sampling period (blue).

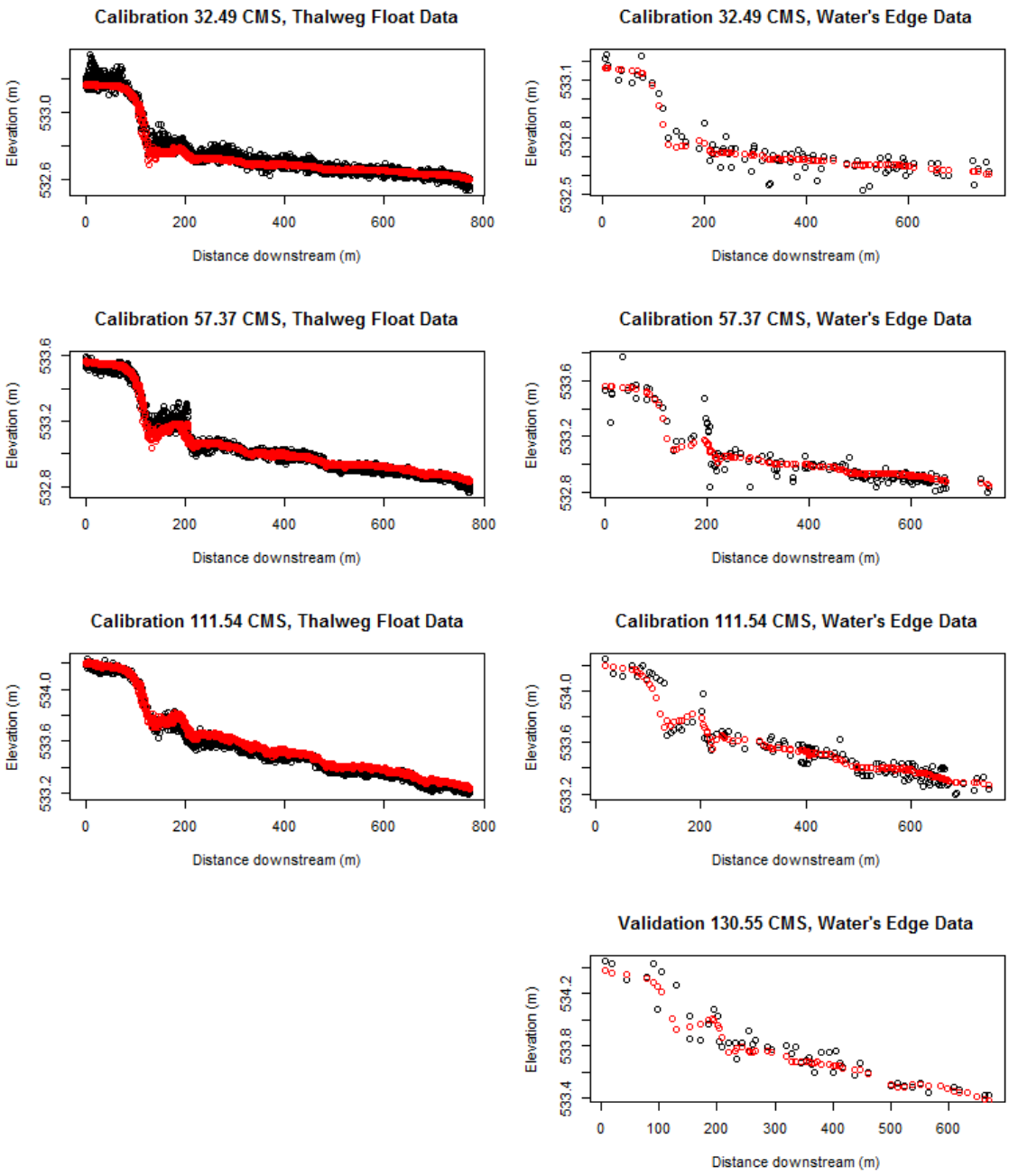

Figure 3. Longitudinal water surface elevation (WSE) plots comparing predicted (red) and observed (black) values at four discharges (32.49, 57.37, 111.54, and 130.55 cms) at the Beaver Creek study site. Model predictions are compared with two sets of observed WSE data: (1) thalweg water surface (L column), and (2) water's edge points (R column).

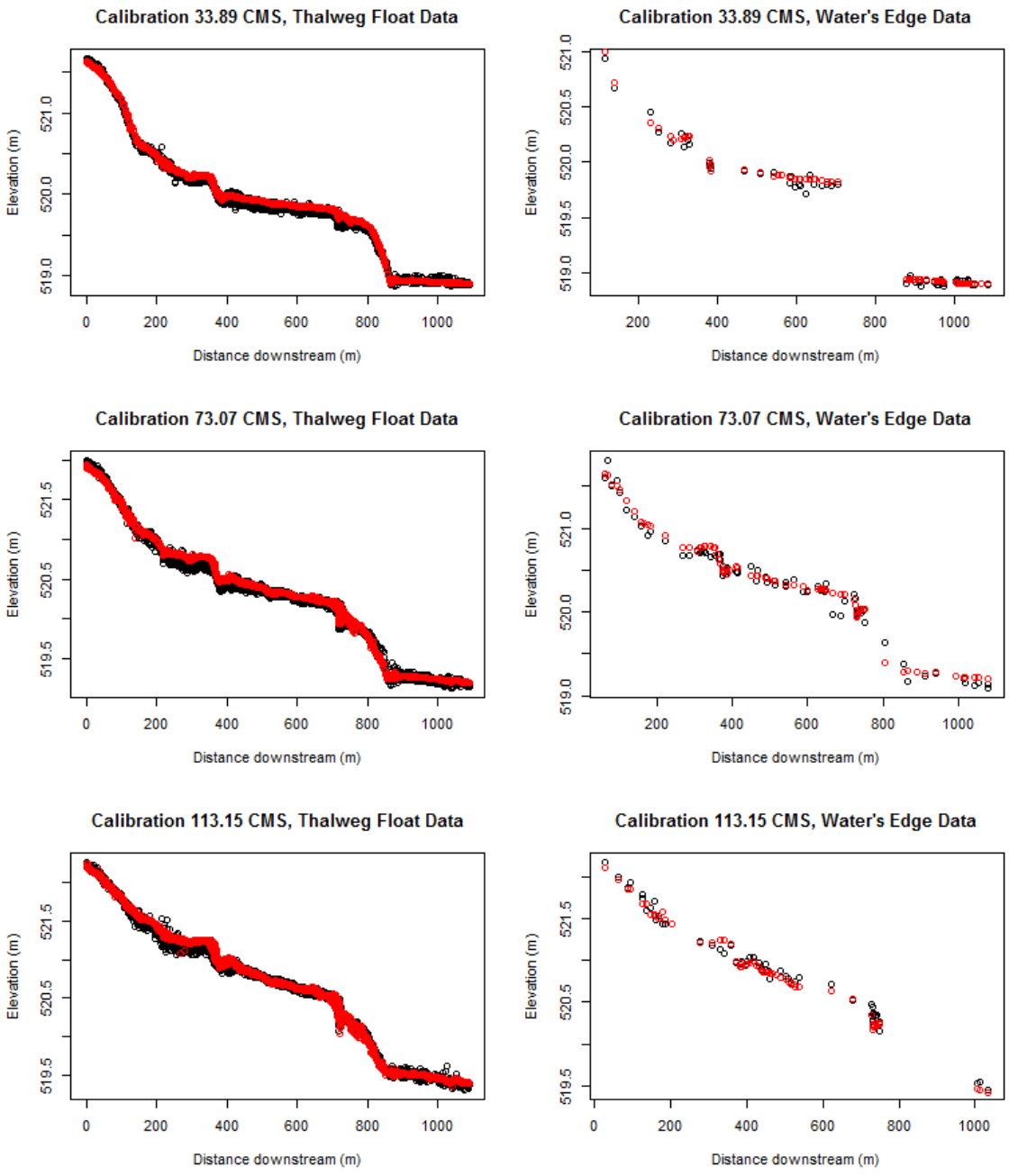

Figure 4. Longitudinal water surface elevation (WSE) plots comparing predicted (red) and observed (black) values at three discharges (33.89, 73.07, 113.15 cms) at the Community Center study site. Model predictions are compared with two sets of observed WSE data: (1) thalweg water surface (L column), and (2) water's edge points (R column).

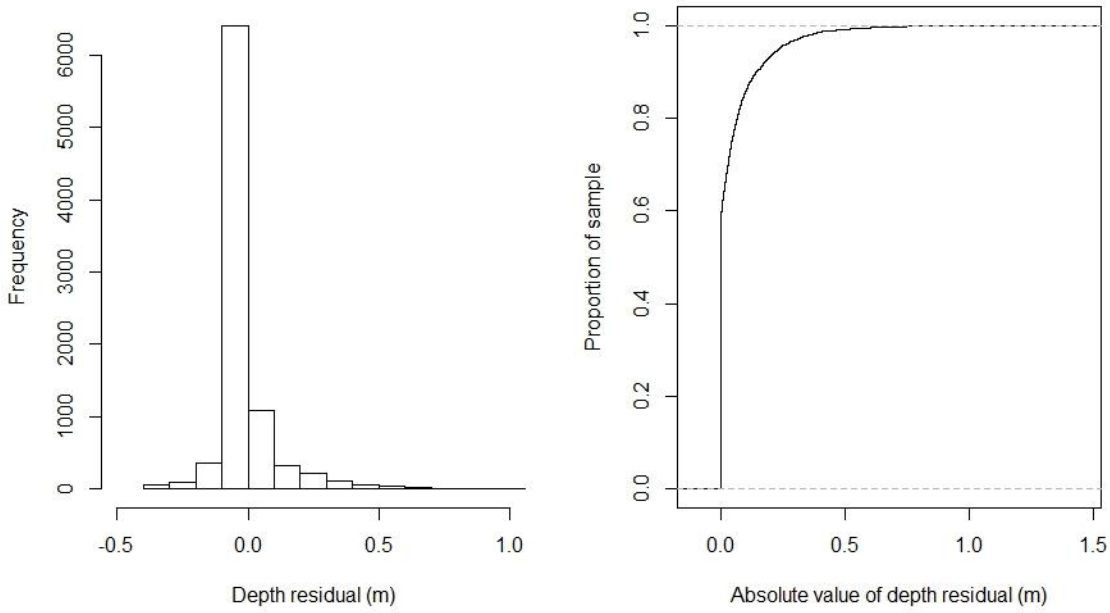

Figure 5. Histogram and cumulative density distribution of depth residuals at all study sites.

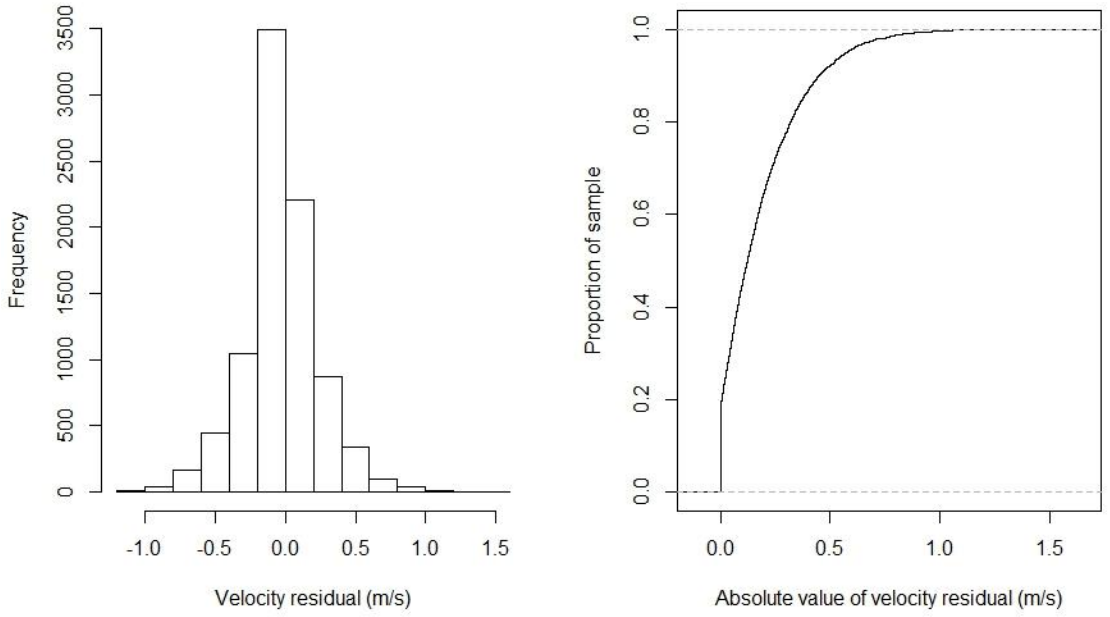

Figure 6. Histogram and cumulative density distribution of velocity residuals at all study sites.

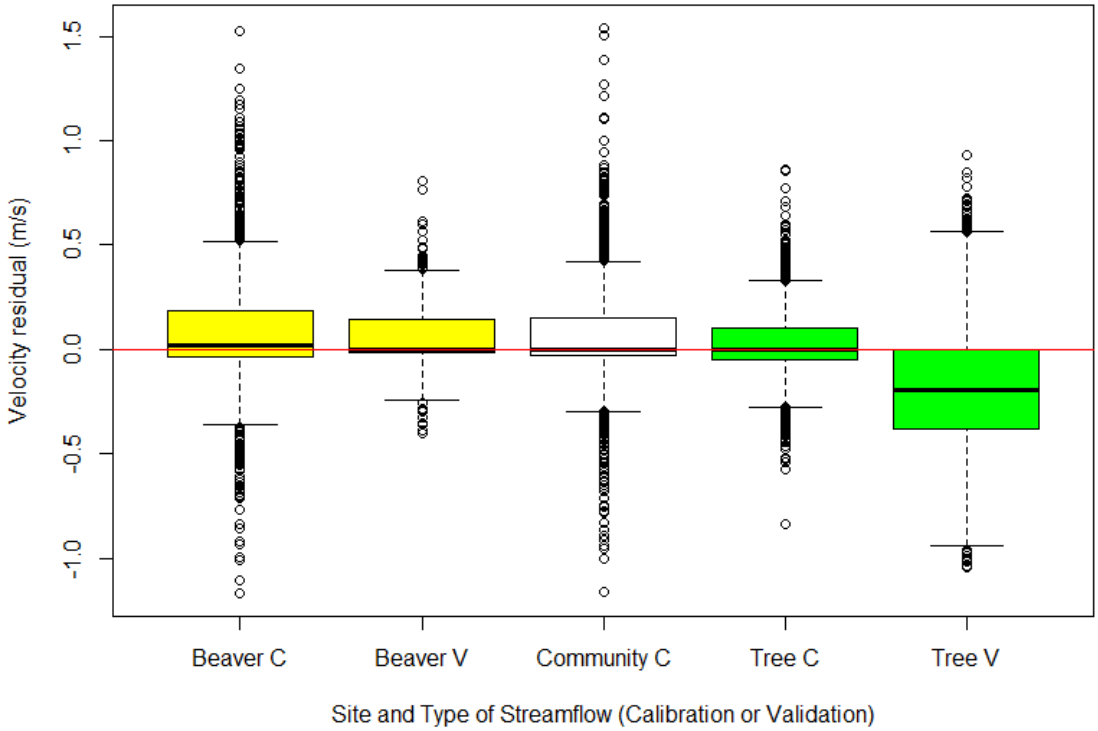

Figure 7. Boxplots of velocity residuals at Beaver Creek (yellow), Community Center (white), and Tree of Heaven study sites (green) for calibration (C) and validation (V) streamflows. Individual outlying data points are displayed as unfilled circles.

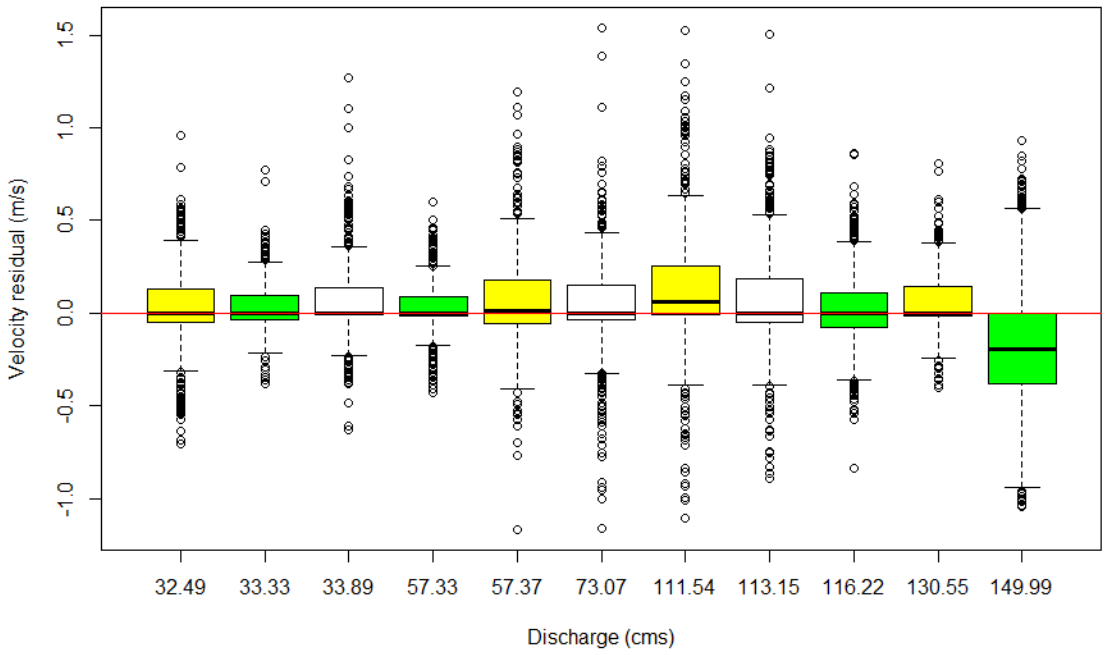

Figure 8. Boxplots of velocity residuals by discharge at study sites Beaver Creek (yellow), Tree of Heaven (green), and Community Center (white). Validation streamflows are 130.55 and 149.99 cms. Individual outlying data points are displayed as unfilled circles.